PRINT ISSN 1119-8362
Electronic ISSN 2659-1499
Full-text Available Online at
https://www.ajol.info/index.php/jasem
https://www.bioline.org.br/ja
J. Appl. Sci. Environ. Manage.
Vol. 28 (10) 3211-3217 October, 2024

Load-Bending Moment Capabilities for 2-Span Continuous Beams under Constant Uniformly Distributed Load

[*1,2]OGBONNA, UK; [2]EBOI, EO

Department of Civil Engineering, University of Benin, Edo State, Nigeria

**Corresponding Author Email:* kingsley.ogbonna@uniben.edu
**ORCID:* https://orcid.org/0009-0006-4594-1826
**Tel: +2348147699692*

Co-authors Email: eboiodion100@gmail.com

ABSTRACT: This paper, investigates the load-bending capabilities for 2-span continuous beams under constant uniformly distributed load (udl) using the slope-deflection method and Staad pro v8i software. The results obtained reveal a standard deviation of 0.012, 0, and 0 for support moments 1, 2, and 3 respectively and coefficient of variation of 1.19%, 0%, and 0% for support moments 1, 2, and 3 respectively. For the span moments 1, and 2 respectively the standard deviation and coefficient of variation obtained were 0.05, 0.02, and, 5.25%, 1.52% respectively. This showed a very good agreement between the staad pro derived model equations and the slope deflection method.

DOI: https://dx.doi.org/10.4314/jasem.v28i10.31

Cite this Article as: OGBONNA, U. K; EBOI, E. O. (2024). Load-Bending Moment Capabilities for 2-Span Continuous Beams under Constant Uniformly Distributed Load. *J. Appl. Sci. Environ. Manage.* 28 (10) 3211-3217

Dates: Received: 07 July 2024; Revised: 15 August 2024; Accepted: 19 August 2024 Published: 05 October 2024

Keywords: moment distribution method; span and support moment coefficient; support moment; span moment; staadpro.

A continuous beam is a multi-span structural element with supports, under the action of external forces, (Kassimali, 2012). The bending moments in a member are needed for design, hence structural engineers apply structural analysis softwares for accurate and timely results, especially when an approximate method is required for preliminary designs (Adam *et al*., 2015; Almayah, 2018). Several design materials containing coefficients are readily available such as Reynolds and Steedman (1999), and the American Wood Council, 2007. Fawzy (2018) examined the effects of the sectional area of a cantilever beam and the maximum length in the control of deflection with the aid of Python 3.4 program. Al-Shammaa and Al-Mamoori, (2021) created a simplified graph for selecting the cross sectional dimensions using a neural network model proposed by Couto (2022). In order to assist engineers in quick and accurate design results, Hong *et al*; 2022 developed an AI-based design approach for predicting various design parameters using design charts. The accuracy was confirmed from structural calculations. Kwan *et al*. (2002); (Shanmukesh *et al*. 2020) established a relationship between the flexural strength and ductility of a simply supported parallelogram-shaped slab, using both mathematical, experimental and finite element procedures. Hong *et al*, (2022) created a forward Lagrange network based artificial neural networks (ANNs) for the optimization of ductile doubly reinforced concrete (RC) beams. To increase the accuracy of the nominal flexural strength capacity of FRP-reinforced beams, Protchenko *et al*. (2021), presented a new empirical coefficient to be

**Corresponding Author Email:* kingsley.ogbonna@uniben.edu
**ORCID:* https://orcid.org/0009-0006-4594-1826
**Tel: +2348147699692*

applied into the ACI 440.1R-15 flexural design technique. Okonkwo and Madu, (2023) made provisions for design tables and charts to lessen design requirements in reinforced concrete beams made of plain and fiber-reinforced geopolymer concrete (GPC, FRGPC). AlHamaydeh and Amin, (2021), developed data on the moment capacities of axially loaded columns. El-Borhamy and Dabaon, (2024) derived a mathematical model to determine the axial critical loads in tapered columns exposed to varying cross sections by applying the Galerkin's method. Charts were put forward in order to elucidate their elastic stability. The objective of this paper is to investigate the load-bending capabilities for 2-span continuous beams under constant uniformly distributed load (udl) using the slope-deflection method and Staad pro v8i software.

MATERIALS AND METHODS

Slope - Deflection Method: Equation 1 is the equation for the Slope Deflection Method analysis of beam structures (Hibbeler, 2015).

$$M_N = 2Ek(2\theta_N + \theta_F - 3\psi) + (FEM)_N \quad 1$$

Where, M_N= Internal near end moment of the span; E,k = Modulus of elasticity, and span stiffness; k =$\frac{I}{L}$; θ_N, θ_F= slopes; ψ = displacement; FEM_N= support fixed end moment.

For fixed ends,

$$(FEM)_N = \frac{wl^2}{12} \quad 2$$

$$\theta_1 = \theta_3 = 0,\ \psi_{12} = \psi_{23} = \psi_{32} = 0,$$

$$w_1 = w_2 = w$$

Through substitutions and applying the equilibrium conditions we obtain the support moments as follows: (Hibbeler, 2015).

$$M_{12} = \frac{wl_2(l_2^2 - l_1^2)}{24(l_1 + l_2)} - \frac{wl_1^2}{12} \quad 3$$

$$M_{21} = \frac{wl_2(l_2^2 - l_1^2)}{12(l_1 + l_2)} + \frac{wl_1^2}{12} \quad 4$$

$$M_{23} = \frac{wl_1(l_2^2 - l_1^2)}{12(l_1 + l_2)} - \frac{wl_2^2}{12} \quad 5$$

$$M_{32} = \frac{wl_1(l_2^2 - l_1^2)}{24(l_1 + l_2)} + \frac{wl_2^2}{12} \quad 6$$

From the free body diagram of each beams span we obtain the span moments as follows (Hibbeler, 2015).

$$M_{span,1} = -M_{12} + \frac{V_1^2 L_1}{2(V_{2L} - V_1)} \quad 7$$

$$M_{span,2} = -M_{23} + \frac{V_{2R}^2 L_2}{2(V_3 - V_{2R})} \quad 8$$

Where $M_{span,1}$ is the first span moment; $M_{span,2}$ is the second span moment; V_{2L} is the node 2 reaction for span 1; V_{2R} is the node 2 reaction for span 2; V_1 is the reaction at node 1; V_3 is the reaction at node 3

Model Staad pro Moment coefficient Formulation: The proposed structure is the two span continuous beam of Lengths L_1 and L_2, with span ratios $\frac{L_1}{L_2}$ ranging from 0.5 to 1.0. Joints 1, and 3 are fixed supports and pinned supported at joint 2 as shown in **fig.1.**

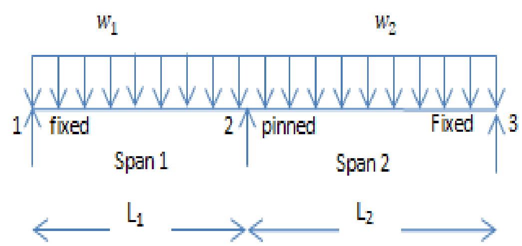

Fig. 1: The 2-span continuous beam model

RESULTS AND DISCUSSIONS

Table 2 displays the average values of the span and support moment coefficients for case 1 to case 11. Due to the nature of the moment coefficients for the node 1 and the span 1 moment coefficients as shown in **Tables 3** as there seem to be a variation in the results of moment coefficients for all example cases, the values of their coefficients are used in plotting the graphs of **Fig.2**, to **Fig.16**. **Table 1** shows the beam dimensions for all eleven cases.

Where; Exp.Case1, L_1 is the length of span 1 for example case 1; Exp.Case2, L_1 is the length of span 1 for example case 2; Exp.Case3, L_1 is the length of span 1 for example case 3; Exp.Case4, L_1 is the length of span 1 for example case 4; Exp.Case5, L_1 is the length of span 1 for example case 5; E and I are constant for both spans.

Table 1: Beam dimensions for all Cases

Parameters	Cases										
	1	2	3	4	5	6	7	8	9	10	11
$\frac{L_1}{L_2}$	0.50	0.55	0.60	0.65	0.70	0.75	0.80	0.85	0.90	0.95	1.00
Exp.Case1, L_1(m)	2.0	2.0	2.0	2.0	2.0	2.0	2.0	2.0	2.0	2.0	2.0
Exp.Case2, L_1(m)	2.5	2.5	2.5	2.5	2.5	2.5	2.5	2.5	2.5	2.5	2.5
Exp.Case3, L_1(m)	3.0	3.0	3.0	3.0	3.0	3.0	3.0	3.0	3.0	3.0	3.0
Exp.Case4, L_1(m)	3.5	3.5	3.5	3.5	3.5	3.5	3.5	3.5	3.5	3.5	3.5
Exp.Case5, L_1(m)	4.0	4.0	4.0	4.0	4.0	4.0	4.0	4.0	4.0	4.0	4.0

A uniformly distributed load of $w_1 = w_2 = 25$KN/m are considered as member loads along span 1 and span 2. Support moment coefficients has been calculated using the equations obtained from the Staad pro analysis for case 1 to case 11 using equations 9, 10, and 11:

$$M_{sppt,1} = w_1 M_{C1} L_1^{\ 2} \quad 9$$

$$M_{sppt,2} = w_2 M_{C2} L_2^{\ 2} \quad 10$$

$$M_{sppt,3} = w_2 M_{C3} L_2^{\ 2} \quad 11$$

Where, $M_{sppt,1}$ is the support moment at node 1; $M_{sppt,2}$ is the support moment at node 2; $M_{sppt,3}$ is the support moment at node 3; w_1 is the udl along span 1; w_2 is the udl along span 2; M_{C1} is the support moment coefficient at node 1; M_{C2} is the support moment coefficient at node 2; M_{C3} is the support moment coefficient at node 3; L_1 is the span length between node 1 and 2; L_2 is the span length between node 2 and 3

Similarly, the span moment coefficient has been calculated from equation 12, and equation 13:

$$M_{span,1} = w_1 M_{C3} L_1^{\ 2} \quad 12$$

$$M_{span,2} = w_2 M_{C4} L_2^{\ 2} \quad 13$$

Where, $M_{span,1}$ is the span moment along span 1; $M_{span,2}$ is the span moment along span 2; w_1 is the udl along span 1; w_2 is the udl along span 2; M_{C3} is the span 1 moment coefficient; M_{C4} is the span 2 moment coefficient.

Application Example: The mathematical equations are applied to ten (10) verification examples in other to validate the accuracy of the equations derived from the staadpro analysis. The parameters for the ten verification examples are shown in **table 3**.

Table 2: Average values of moment coefficients

CASE	$\frac{L_1}{L_2}(r_n)$	NODE 1	NODE 2	NODE 3	SPAN 1	SPAN 2
1	0.50	0.010	0.062	0.094	0.025	0.047
2	0.55	0.028	0.062	0.094	0.024	0.047
3	0.60	0.042	0.063	0.093	0.025	0.046
4	0.65	0.053	0.064	0.093	0.028	0.047
5	0.70	0.061	0.065	0.092	0.031	0.046
6	0.75	0.067	0.067	0.091	0.033	0.046
7	0.80	0.072	0.070	0.090	0.035	0.045
8	0.85	0.076	0.073	0.088	0.037	0.045
9	0.90	0.079	0.076	0.087	0.039	0.043
10	0.95	0.081	0.079	0.085	0.040	0.043
11	1.00	0.083	0.083	0.083	0.042	0.042

Table 3: Parameters for the verification examples

Verification Examples	$\frac{L_1}{L_2}$	L_1 *(m)*	L_2 *(m)*	$\frac{(L_2 - L_1)\%}{L_2}$	(ΔL) *(m)*	$L_1 - \Delta L$ *(m)*	$\frac{(L_1 - \Delta L)\%}{L_1}$
V1	0.504	2.90	5.76	49.65	2.86	0.04	1.38
V2	0.508	3.00	5.91	49.24	2.91	0.09	3.00
V3	0.508	3.10	6.10	49.18	3.00	0.10	3.23
V4	0.509	4.20	8.25	49.09	4.05	0.15	3.57
V5	0.523	3.15	6.02	47.67	2.87	0.28	8.89
V6	0.585	4.35	7.44	41.53	3.09	1.26	28.97
V7	0.612	3.85	6.29	38.79	2.44	1.41	36.62
V8	0.755	3.65	4.83	24.43	1.18	2.47	67.67
V9	0.925	4.10	4.43	7.45	0.33	3.77	91.95
V10	0.955	3.75	3.93	4.58	0.18	3.57	95.20

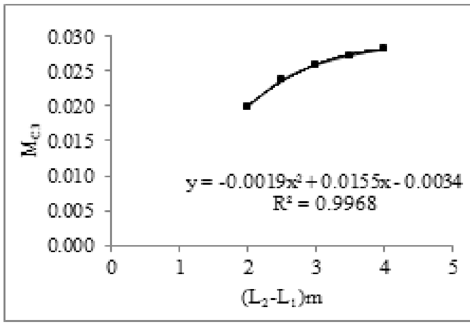

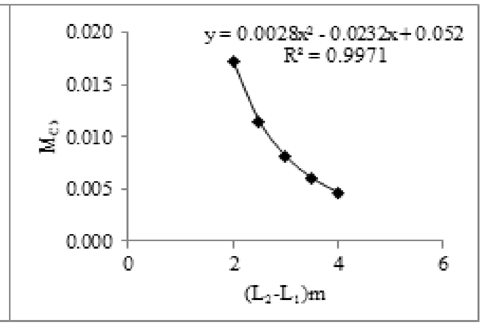

Fig.2: M_{C3} vs $(L_2 - L_1)$ for case 1

Fig.3: M_{C3} vs $(L_2 - L_1)$ for case 1

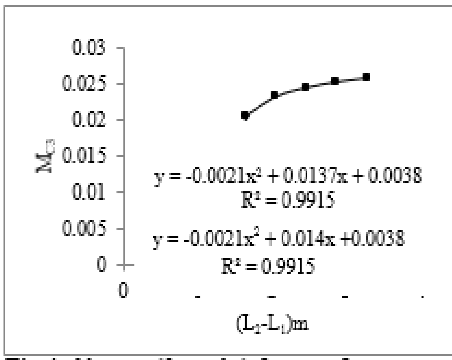

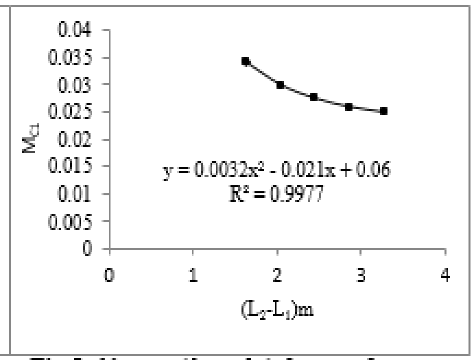

Fig.4: M_{C3} vs $(L_2 - L_1)$ for case 2

Fig.5: M_{C3} vs $(L_2 - L_1)$ for case 2

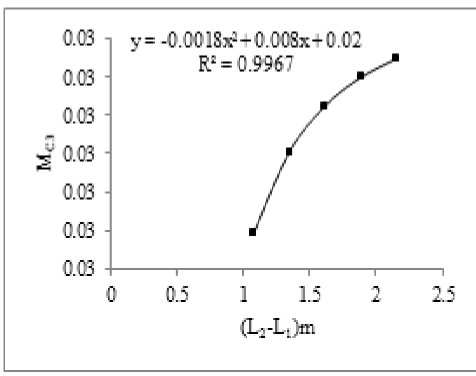

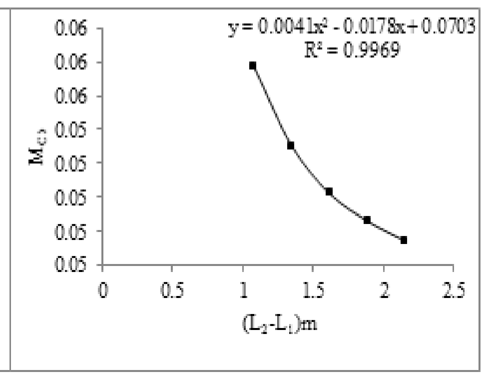

Fig.6: M_{C3} vs $(L_2 - L_1)$ for case 3

Fig.7: M_{C3} vs $(L_2 - L_1)$ for case 3.

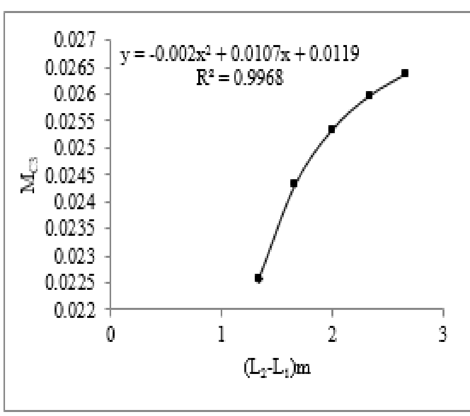

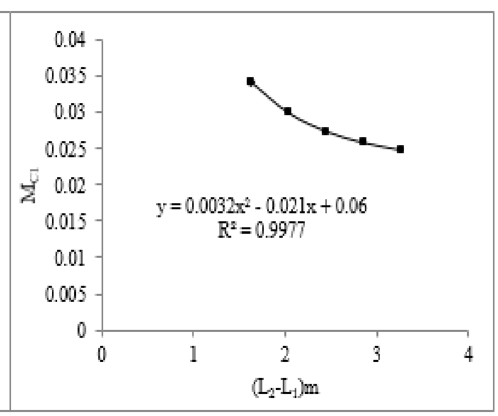

Fig.9: M_{C3} vs $(L_2 - L_1)$ for case 4

Fig.10: M_{C3} vs $(L_2 - L_1)$ for case 4

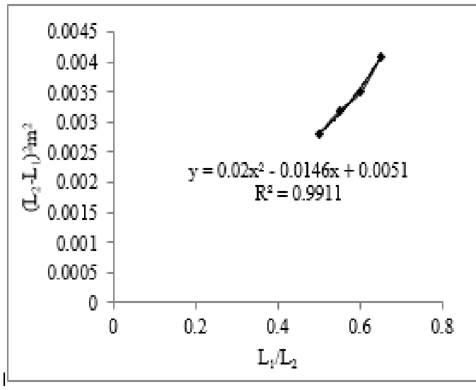

Fig.11: $(L_2 - L_1)^2$ vs $\frac{L_1}{L_2}$ for support coefficients.

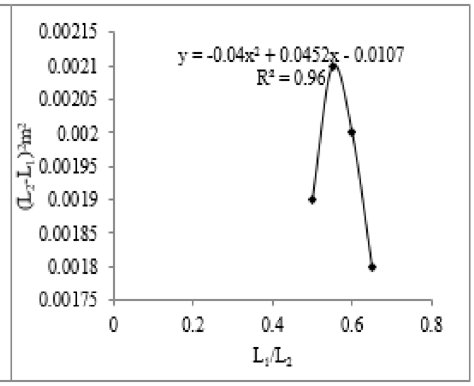

Fig.12: $(L_2 - L_1)^2$ vs $\frac{L_1}{L_2}$ for span coefficients.

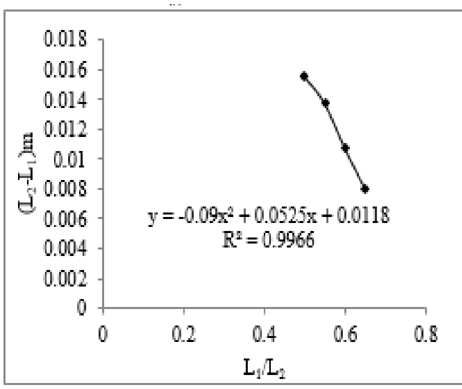

Fig.13: $(L_2 - L_1)^2$ vs $\frac{L_1}{L_2}$ for support coefficients.

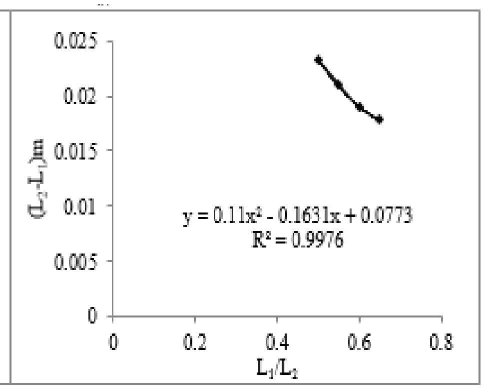

Fig.14: $(L_2 - L_1)^2$ vs $\frac{L_1}{L_2}$ for span coefficients.

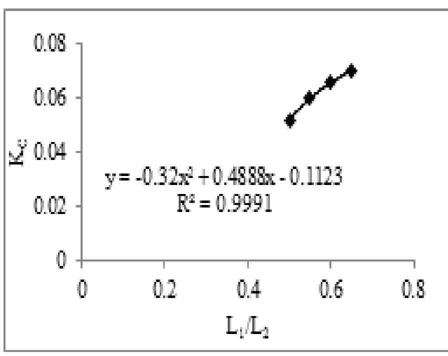

Fig.15: (K_C) vs $\frac{L_1}{L_2}$ for supports.

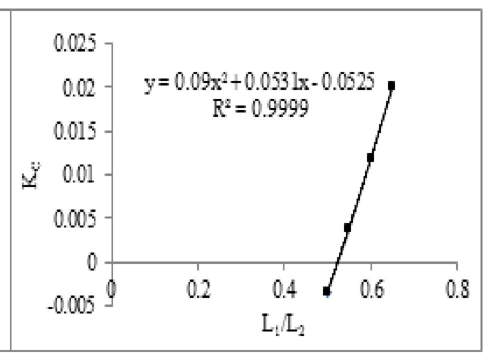

Fig.16: (K_C) vs $\frac{L_1}{L_2}$ for spans

The following equations are obtained:

$$M_{C1,Case1.sppt} = 0.0028(L_2 - L_1)^2 - 0.0232(L_2 - L_1) + 0.052 \quad 14$$

$$M_{C1,Case2,sppt} = 0.0032(L_2 - L_1)^2 - 0.0210(L_2 - L_1) + 0.060 \quad 15$$

$$M_{C1,Case3,sppt} = 0.0035(L_2 - L_1)^2 - 0.0189(L_2 - L_1) + 0.066 \quad 16$$

$$M_{C1,Case4,sppt} = 0.0041(L_2 - L_1)^2 - 0.0178(L_2 - L_1) + 0.070 \quad 17$$

$$M_{C1,Case1,span} = -0.0019(L_2 - L_1)^2 + 0.0155(L_2 - L_1) - 0.0034 \quad 18$$

$$M_{C1,Case2,span} = -0.0021(L_2 - L_1)^2 + 0.0137(L_2 - L_1) + 0.0034 \quad 19$$

$$M_{C1,Case3,span} = -0.0020(L_2 - L_1)^2 + 0.0107(L_2 - L_1) + 0.0119 \quad 20$$

$$M_{C1,Case4,span} = -0.0018(L_2 - L_1)^2 + 0.0080(L_2 - L_1) + 0.0200 \quad 21$$

$Where$; $M_{C1,case1,sppt}$ is the support moment coefficient for case 1; $M_{C1,case2,sppt}$ is the support moment coefficient for case 2; $M_{C1,case3,sppt}$ is the support moment coefficient for case 3; $M_{C1,case4,sppt}$ is the support moment coefficient for case 4; $M_{C1,case1,span}$ is the span moment coefficient for case 1; $M_{C1,case2,span}$ is the span moment coefficient for case 2; $M_{C1,case3,span}$ is the span moment coefficient for case 3; $M_{C1,case4,span}$ is the span moment coefficient for case 4.

The following relationships are extracted from the graphs:

$$(L_2 - L_1)^2{}_{sppt} = 0.023r^2 - 0.014r + 0.0051 \quad 22$$

$$(L_2 - L_1)_{sppt} = 0.11r^2 - 0.1631r + 0.0773 \quad 23$$

$$(L_2 - L_1)^2{}_{span} = -0.04r^2 + 0.0452r - 0.0107 \quad 24$$

$$(L_2 - L_1)_{span} = 0.09r^2 + 0.0525r + 0.0118 \quad 25$$

$$K_{C\,span} = 0.09r^2 + 0.0531r - 0.0525 \quad 26$$

$$K_{C\,sppt} = -0.32r^2 + 0.4888r - 0.1123 \quad 27$$

Where K_C is the coefficient of the constants.

Where equations 22 and 23 are for node 1 support, equations 24 and 25 are for span 1, equation 26 is for the span 1, and equation 27 is for node 1 support. Substituting equations 22, 23, 24, 25, 26, and 27 into equations 14,15,16,17,18,19, 20, and 21 gives the following equations 28, and 29 for node 1 and span 1 moment coefficients to two significant figures:

$$M_{C1,sppt} = [(0.02r^2 - 0.146r + 0.0051)(L_2 - L_1)^2] - [(0.11r^2 - 0.163r + 0.077)(L_2 - L_1)] + [(0.489r - 0.32r^2 - 0.112)] \quad 28$$

$$M_{C1,span} = [(-0.09 + 0.053r + 0.012)(L_2 - L_1)] - [(-0.04r^2 + 0.045r - 0.011)(L_2 - L_1)^2] - [(0.053r + 0.09r^2 - 0.053)] \quad 29$$

Where $M_{C1,sppt}$ = moment coefficient for node1; $M_{C1,span}$ = moment coefficient for span 1, and $r = \frac{L_1}{L_2}$

The moment coefficients using equations 28 and 29 have also been inputed into a computer-based spreadsheet application built in Microsoft Excel. **Table 4**, and **table 5** show that the coefficient of variation for support moments 1, 2, and 3 was 1.19%, 0%, and 0%, while the standard deviation for those moments was 0.012, 0, and 0. The standard deviation and coefficient of variation for span moments 1 and 2, respectively, were 0.05 and 0.02, or 5.25% and 1.52%. This demonstrated a very high degree of agreement between the slope deflection equation and the model equations generated using Staad Pro.

Table 4: Comparisms of span moment coefficients for Slope-deflection method and the staad pro analysis model equation

Verification Examples	M_{span1} (KNm)	P_{span1} (KNm)	M_{span2} (KNm)	P_{span2} (KNm)	$\frac{M_{Span2}}{P_{Span2}}$	$\frac{M_{Span2}}{P_{Span2}}$
V1	6.48	6.20	39.28	38.98	0.96	0.99
V2	6.84	6.71	41.36	41.04	0.98	0.99
V3	7.29	7.30	44.06	43.72	0.99	0.99
V4	13.33	15.62	80.59	79.97	0.85	0.99
V5	7.22	7.33	42.94	42.62	0.99	0.99
V6	13.19	14.61	65.22	64.28	0.90	0.99
V7	10.55	11.13	46.55	46.01	0.95	0.99
V8	11.38	12.96	26.75	26.59	0.88	0.99
V9	16.77	16.81	21.19	22.59	0.99	0.94
V10	14.29	14.41	16.41	16.58	0.99	0.99
				Mean	0.95	0.99
				SD	0.05	0.02
				Cov (%)	5.25	1.52

Table 5: Comparisms of support moment coefficients for Slope-deflection method and the staad pro analysis model equation

Verification Examples	$M_{1,sppt}$ (KNm)	$P_{1,sppt}$ (KNm)	$M_{2,sppt}$ (KNm)	$P_{2,sppt}$ (KNm)	$M_{3,sppt}$ (KNm)	$P_{3,sppt}$ (KNm)	$\frac{M_{1,Sppt}}{P_{1,Sppt}}$	$\frac{M_{2,Sppt}}{P_{2,Sppt}}$	$\frac{M_{3,Sppt}}{P_{3,Sppt}}$
V1	0.36	1.56	51.84	51.43	77.76	77.97	0.23	0.99	0.99
V2	0.83	1.89	54.58	54.14	81.86	82.08	0.44	0.99	0.99
V3	0.96	1.89	58.15	57.68	87.21	87.44	0.51	0.99	0.99
V4	1.95	1.11	106.36	105.50	159.52	159.95	0.57	0.99	0.99
V5	2.65	3.47	56.72	56.23	85.00	85.25	0.76	0.99	0.99
V6	15.52	15.32	87.23	86.40	129.18	129.25	0.99	0.99	0.99
V7	14.89	15.14	62.87	62.53	92.24	92.01	0.98	0.99	0.99
V8	21.79	22.65	39.68	39.27	53.19	52.88	0.96	0.99	0.99
V9	33.49	33.62	38.09	38.31	42.35	42.24	0.99	0.99	0.99
V10	28.57	28.13	30.74	30.45	32.81	32.38	0.99	0.99	0.99
			Mean = (V6 to V10)				0.98	0.99	0.99
			Standard Deviation=(V6 to V10)				0.012	0.00	0.00
			Coefficient of variation(%) = (V6 to V10)				1.19	0.00	0.00

Conclusion: Using the staad pro software, the moment coefficients for a two-span continuous beam under a constant, evenly distributed load over spans 1 and 2 have been derived. As a result, a mathematical equation that illustrates the model equations derived from this parametric study is used to solve moment coefficient problems in the ten example verification. For quick design and design checks, practicing engineers might find value in using the model equations.

Declaration of Conflict of Interest: The authors declare no conflict of interest.

Data availability statement: Data are available upon request from the first author or corresponding author.

REFERENCES

AlHamaydeh, M; Amin, F (2021). Data Descriptor Data for Interaction Diagrams of Geopolymer FRC Slender Columns with Double-Layer GFRP and Steel Reinforcement. *Data*. 6(43): 1-7

Al-Shammaa, AK; Al-Mamoori, SK (2021). A Design Chart for Optimum Dimensions of Reinforced Concrete Cantilever Beams. *IOP Conference Series: Mat. Sci. Engineer.* 1094: 1-11. doi:10.1088/1757-899X/1094/1/012023

American wood council (2007). Beams formulas with shear and moment diagrams. Ame. Fore and paper assoc., inc, Design aids No. 6.

Couto, C (2022). Neural network models for the critical bending moment of uniform and tapered beams. *Struct.* 41:1746-1762.

El-Borhamy, M; Dabaon, MA. 2024. An application of stability charts to prediction of buckling instability in tapered columns via Galerkin's method. *Disc. Appl. Sci*. 6:1-14. https://doi.org/10.1007/s42452-024-05740-5.

Fawzy, SA (2018). Design charts for simple and one continuous side paneled reinforced concrete beams. *Procedure of the 12th International Conference on Civil and Architectural Engineering ICCAE-12.*

Hibbeler, R.C (2015). Structural analysis. *Pearson education Ltd., London.*

Hong, WK; Nguyen, VT; Nguyen, MC (2022). Artificial intelligence-based novel design charts for doubly reinforced concrete beams. *J. Asian Arch. Build. Eng.* 21(4):1497-1519.

Hong, WK; Nguyen, VT; Nguyen, MC (2022). Optimizing reinforced concrete beams cost based on AI-based lagrange functions. *Build. Struct. Mat.* 21(6): 2426-2443.

Kassimali, A (2012). 'Matrix Analysis of Structures. Second edition., Souther Illinois University-Carbondale, Cenage learning.

Kwan, AKH; Ho, JCM; Pam, H.J (2002). Flexural strength and ductility of reinforced concrete beams. *Proceedings of the institution of civil Engineers-Structures and Buildings.* 152(4):361-369. *http://doi.org/10.1680/stub.2002.152.4.361*.

Okonkwo, V; Madu, SJ; 2023. Formulation of design tables and charts for design of reinforced concrete Beams. A project submitted In partial fulfilment of the requirement for the award of bachelor of Engineering degree (B.Eng) in the department of Civil Engineering, Faculty of Engineering, Nnamdi Azikiwe University, Awka, Nigeria.

Protchenko, K; Le´sniak, P; Szmigiera, E; Urba ´nski; M. 2022.New Model for Analytical Predictions on the Bending Capacity of Concrete Elements Reinforced with FRP Bars. *Mat.* 14 (693): 1-17. https:// doi.org/10.3390/ma14030693.

Shanmukesh, DV; Gupta, MRVS; Naidu, KA (2020). Development of design charts of a parallelogram shaped slab by using yield line methodology. *J. Mukt. Shabd.* X(III): 80-93.